Reactive intercalation and oxidation at the buried graphene-germanium interface

Philipp Braeuninger-Weimer (ID), Oliver Burton, Robert S. Weatherup (ID), Ruizhi Wang, Pavel Dudin, Barry Brennan, Andrew J. Pollard, Bernhard C. Bayer, Vlad P. Veigang-Radulescu, Jannik C. Meyer, Billy J. Murdoch, Peter J. Cumpson, and Stephan Hofmann (ID)

View Online   Export Citation   CrossMark

ARTICLES YOU MAY BE INTERESTED IN

Control of etch pit formation for epitaxial growth of graphene on germanium
Journal of Applied Physics 126, 085306 (2019); https://doi.org/10.1063/1.5108774

Investigation of surface reactions in metal oxide on Si for efficient heterojunction Si solar cells
APL Materials 7, 071106 (2019); https://doi.org/10.1063/1.5100884

Self-assembly and properties of domain walls in BiFeO$_3$ layers grown via molecular-beam epitaxy
APL Materials 7, 071101 (2019); https://doi.org/10.1063/1.5103244

ORDER PRINT EDITION

AIP Conference Proceedings
The 18th International Conference on Positron Annihilation

Reactive intercalation and oxidation at the buried graphene-germanium interface

View Online   Export Citation   CrossMark

Philipp Braeuninger-Weimer,[1,a] (iD) Oliver Burton,[1] Robert S. Weatherup,[2,3] (iD) Ruizhi Wang,[1] Pavel Dudin,[4] Barry Brennan,[5] Andrew J. Pollard,[5] Bernhard C. Bayer,[6,7] Vlad P. Veigang-Radulescu,[1] Jannik C. Meyer,[6] Billy J. Murdoch,[8,b] Peter J. Cumpson,[8] and Stephan Hofmann[1,a] (iD)

AFFILIATIONS

[1] Department of Engineering, University of Cambridge, Cambridge CB3 0FA, United Kingdom
[2] The University of Manchester at Harwell, Diamond Light Source, Harwell Campus, Didcot OX11 0DE, United Kingdom
[3] School of Chemistry, University of Manchester, Oxford Road, Manchester M13 9PL, United Kingdom
[4] Diamond Light Source, Didcot OX11 0DE, United Kingdom
[5] National Physical Laboratory, Hampton Rd, Teddington, Middlesex TW11 0LW, United Kingdom
[6] Faculty of Physics, University of Vienna, Boltzmanngasse 5, A-1090 Vienna, Austria
[7] Institute of Materials Chemistry, Vienna University of Technology (TU Wien), Getreidemarkt 9/165, A-1060 Vienna, Austria
[8] National EPSRC XPS Users' Service (NEXUS), School of Mechanical and Systems Engineering, Newcastle University, Newcastle Upon Tyne NE1 7RU, United Kingdom

[a] Authors to whom correspondence should be addressed: philipp.braeuninger@gmail.com and sh315@cam.ac.uk
[b] Present address: School of Science, RMIT University, VIC 3001, Melbourne, Australia.

ABSTRACT

We explore a number of different electrochemical, wet chemical, and gas phase approaches to study intercalation and oxidation at the buried graphene-Ge interface. While the previous literature focused on the passivation of the Ge surface by chemical vapor deposited graphene, we show that particularly via electrochemical intercalation in a 0.25 N solution of anhydrous sodium acetate in glacial acetic acid, this passivation can be overcome to grow GeO_2 under graphene. Angle resolved photoemission spectroscopy, Raman spectroscopy, He ion microscopy, and time-of-flight secondary ion mass spectrometry show that the monolayer graphene remains undamaged and its intrinsic strain is released by the interface oxidation. Graphene acts as a protection layer for the as-grown Ge oxide, and we discuss how these insights can be utilized for new processing approaches.

INTRODUCTION

Heterogeneous materials' integration and interface control are key challenges for integrated device technology. 2D layered materials such as graphene offer a versatile platform to create a wide range of new heterostructures, as highlighted by the recent literature on the so-called van der Waals heterostructures.[1–3] The importance of interface effects between 2D and 3D materials is only starting to emerge. Examples in the context of 2D material manufacturing include growth by scalable chemical vapor deposition (CVD),[4–8] transfer,[9–12] contacts,[13] encapsulation of 2D device channels[14–17] or the wettability,[18–20] remote epitaxy,[21] and surface and corrosion protection effects that 2D materials can provide for 3D materials.[22,23] Intercalation at the graphene-metal interface has been widely studied as a means of tuning interaction strength, and the selective oxidation of the metal surface beneath graphene has been introduced as a route to facilitate graphene transfer.[10,24–26] It has been recently shown that direct CVD of graphene is possible on Ge (100), (111), and (110) surfaces.[27–32] This offers a route for metal-contamination free graphene CVD, akin to graphene growth on SiC substrates.[33–37] As-grown monolayer graphene has been reported to provide stabilization and passivation of the Ge surfaces.[38,39] In contrast to

the native oxide of Si which forms an excellent interface with Si and provides good passivation, GeO_2, the native oxide of Ge, is water soluble, i.e., offers poor protection, and forms a poor interface with Ge.[40–43] Analogous to prior work on SiC based graphene growth, hydrogen intercalation at the graphene-Ge interface has been studied.[36,44–46] The motivation being to preserve and tune the graphene-Ge interface for use in processes and devices where graphene directly supported on Ge is desired. However, for many applications, the opposite is of interest, i.e., the complete decoupling or removal of graphene from Ge, particularly via the formation of a new layer at the buried graphene-Ge interface. This remains largely unexplored.

Here, we study oxidation at the buried graphene-Ge interface as a simple model reaction to explore the effect of monolayer graphene coverage on the Ge. It is well known that an uncovered Ge surface can be oxidized by immersion in nitric acid (HNO_3)[42,47–50] or hydrogen peroxide (H_2O_2).[51] However, the water present in aqueous solutions of nitric acid and hydrogen peroxide leads to the simultaneous dissolution of the GeO_2.[41,47] The Pourbaix diagram of Ge, which maps out the stable (equilibrium) phases of an aqueous electrochemical system, highlights only a very narrow region where Ge oxides are stable (as GeO) which lies entirely outside of the electrochemical stability window of water.[41] Thus, the oxidation of pristine Ge through immersion in aqueous liquids is accompanied by simultaneous dissolution of the Ge oxide.[52] Nonaqueous Ge oxidation is possible by electrochemical oxidation with the formation of Ge oxide layers demonstrated using glacial acetic acid and anhydrous sodium acetate as electrolyte.[53] We show here how the result of such reactions can change in the presence of a monolayer of graphene. Through intercalation mediated reactive interface oxidation, even wet chemical approaches can be used to grow thick Ge oxide layers at the buried interface protected by graphene. Graphene acts as an ultrathin capping layer in analogy to the previous reported use of thicker capping layers and oxidation at capped Ge oxide interfaces.[54–56] We explore a number of different electrochemical, wet chemical, and gas phase approaches to oxidation and also nitridation. Using an electrochemical oxidation approach, the graphene monolayer remains undamaged, while a thick Ge oxide layer can be grown at the buried interface. The roughness of this oxide leaves the graphene layer partly free-standing, and the CVD induced strain in the graphene layer is released. We show detailed characterization of this via angle resolved photoemission spectroscopy (ARPES), Raman spectroscopy, He ion microscopy, and time-of-flight secondary ion mass spectrometry (ToF-SIMS) and discuss how this knowledge can be utilized for new processing approaches.

RESULTS AND DISCUSSION

Figure 1 schematically shows the process flow and the separate reaction pathways that we focus on. We use CVD to directly grow monolayer graphene on Ge wafers (see the supplementary material, for further details). As a model system, we specifically focus on the Ge(110) orientation, motivated by the prior literature reporting the lowest graphene defect density for this orientation.[27,32] Our CVD conditions result in an average graphene domain size of the order of few micrometer (see the supplementary material, Fig. S1), and transmission electron microscopy (TEM) analysis indicates that
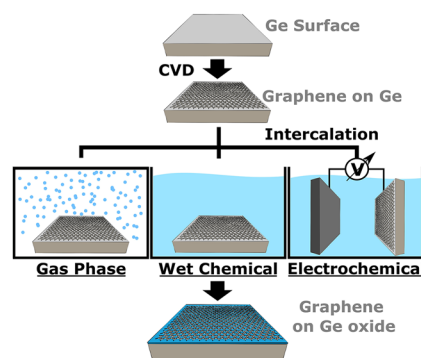

FIG. 1. Process flow overview: Continuous, monolayer graphene is grown by CVD on untreated Ge wafers, and intercalation/interface oxidation is explored via gas phase, wet chemical, and electrochemical processes.

there are predominantly two graphene domain orientations present, rotated by 30° with respect to each other, consistent with the previous literature.[27,31,32,57,58] For Ge, it is established that the difference in oxidation rates for different surface orientations is relatively small;[59,60] hence, we expect the oxidation results on other Ge surfaces to be similar. As we show below, our CVD-grown monolayer graphene film inhibits Ge oxidation in ambient air, in line with previous reports.[38,39] The question we focus on here is if this passivation can be overcome without damaging the graphene layer. For this, we consider three separate pathways to interface oxidation (see Fig. 1): gas phase, wet chemical, and electrochemical.

Gas phase approaches, where the graphene/Ge sample was exposed to oxygen- or ammonia-containing atmospheres at 400–750 °C, were performed (more information in the supplementary material, Sec. III), but the high temperatures required and reactive gas species resulted in graphene damage or complete graphene removal without intercalation. Wet chemical processes using nitric acid condensation or hydrogen peroxide floating for 2 h are successful in growing interfacial oxides (see the supplementary material, Sec. III), but obtaining homogeneous coverage over large areas is challenging because of the instability of the Ge oxide in aqueous liquids. Thus, we focus here on the electrochemical approach in a nonaqueous solution, which overcomes the problem of Ge oxide instability while providing the electrochemical potential to drive intercalation and interface oxidation. Our results regarding the gas phase and wet chemical reactive intercalation are shown in the supplementary material.

Electrochemical intercalation is performed in a simple voltaic cell. The graphene-Ge sample was immersed in a nonaqueous solution of acetic acid and sodium acetate at 1 V for 6–24 h (see the section titled "Methods"). We employ nanoresolution angle resolved photoemission spectroscopy (nanoARPES) to probe the electronic structure of graphene and gain insights into the interaction of the graphene layer with Ge(110) and with the electrochemically grown interfacial oxide. NanoARPES further allows us to locally probe the photoemission spectrum of Ge, i.e., to probe the oxidation state of Ge under graphene. Intercalation can result in electronic decoupling of graphene from the substrate, as is the case for strongly interacting substrates (e.g., SiC, Ni, and Ru)[36,61,62] where graphene's linear dispersion near the K-point can be recovered, or for more weakly

interacting substrates where charge-transfer from the substrate may be reduced (e.g., Pt and Cu).[63,64] On the other hand, charge transfer from intercalated oxygen species can cause a shift in the graphene Fermi level.[22,64,65] The ARPES spectra of as-grown graphene on Ge(110) [Fig. 2(a)] exhibit a linear dispersion near the Dirac points with a Fermi level shift of -50 ± 25 meV, corresponding to graphene with very weak p-type doping. Note that all grown and intercalated samples were stored in air for several weeks before measurement and *in situ* annealed in the ARPES chamber (see the section titled "Methods"). At the same location, the photoemission spectrum in the binding energy range of 28–34 eV shows two peaks corresponding to the $Ge3d_{5/2}$ (29.3 eV) and $Ge3d_{3/2}$ (29.8 eV)[66] core levels [Fig. 2(c)]. The spectrum shows no contributions of GeO or GeO_2 peaks, highlighting the passivating effect of the graphene monolayer at ambient conditions in line with the previous literature.[38,39] After electrochemical intercalation for 6 h, the graphene ARPES spectra are almost unchanged [Fig. 2(b)]. We only observe a small shift in the graphene Femi level to -80 ± 25 meV, corresponding to weak p-type doping. However, after electrochemical intercalation, the photoemission spectrum shows a significant change and the emergence of additional peaks at 30.9 eV and 32.5 eV corresponding to GeO and GeO_2, respectively [Fig. 2(c)].[66] This confirms the successful growth of an interfacial oxide layer whilst largely preserving the electronic structure of the graphene.

Figure 3 shows the Raman spectra before and after such electrochemical Ge oxidation. Following intercalation, the intensities of the graphene 2D and G peaks increase by ~45 and ~30 times, respectively [Fig. 3(a)]. The 2D peak shifts by approximately 20 cm^{-1}, from ~2700 cm^{-1} to ~2680 cm^{-1} after electrochemical intercalation. A Raman peak at 444 cm^{-1} is observed after intercalation [Fig. 3(c)], which we assign to trigonal GeO_2.[67] Raman mapping confirms that such intercalation does not result in a significant increase in the graphene D peak (see the supplementary material, Fig. S4).

In line with previous reports,[38] the Raman signal intensity of as-grown monolayer graphene on Ge(110) is comparatively weak and long accumulation times are required to resolve the Raman signature (see the supplementary material, Fig. S5). Reactive intercalation and dielectric formation result in a marked increase in the graphene Raman intensity, and our data suggest that this is due to the following effects. Electronic screening of the substrate has been shown to reduce the graphene Raman signal intensity. In particular, when the graphene layer is in close contact with a metallic substrate, as is the case with direct CVD synthesis, this effect is pronounced.[68] In the case of graphene on Pt, a similar Raman enhancement was observed upon intercalation.[69] Second, it is well established that the interference on a Si/SiO$_2$ stack can enhance not only the optical contrast of graphene[73] but also the graphene Raman signal intensity.[74,75] Thus, also upon formation of an interfacial Ge oxide layer, a graphene Raman signal enhancement (compared to the as-grown case of graphene on Ge) can be expected.[25,76] Very strong coupling between graphene and the substrate can also result in hybridization of the graphene electronic bands (e.g., Ru[70] and Ni[71]) and consequently a loss of the resonant condition for Raman scattering.[72] However, this effect can be excluded in this case as our ARPES data reveal no such perturbation of the graphene Dirac cone near the Fermi level [Figs. 2(a) and 2(b)].
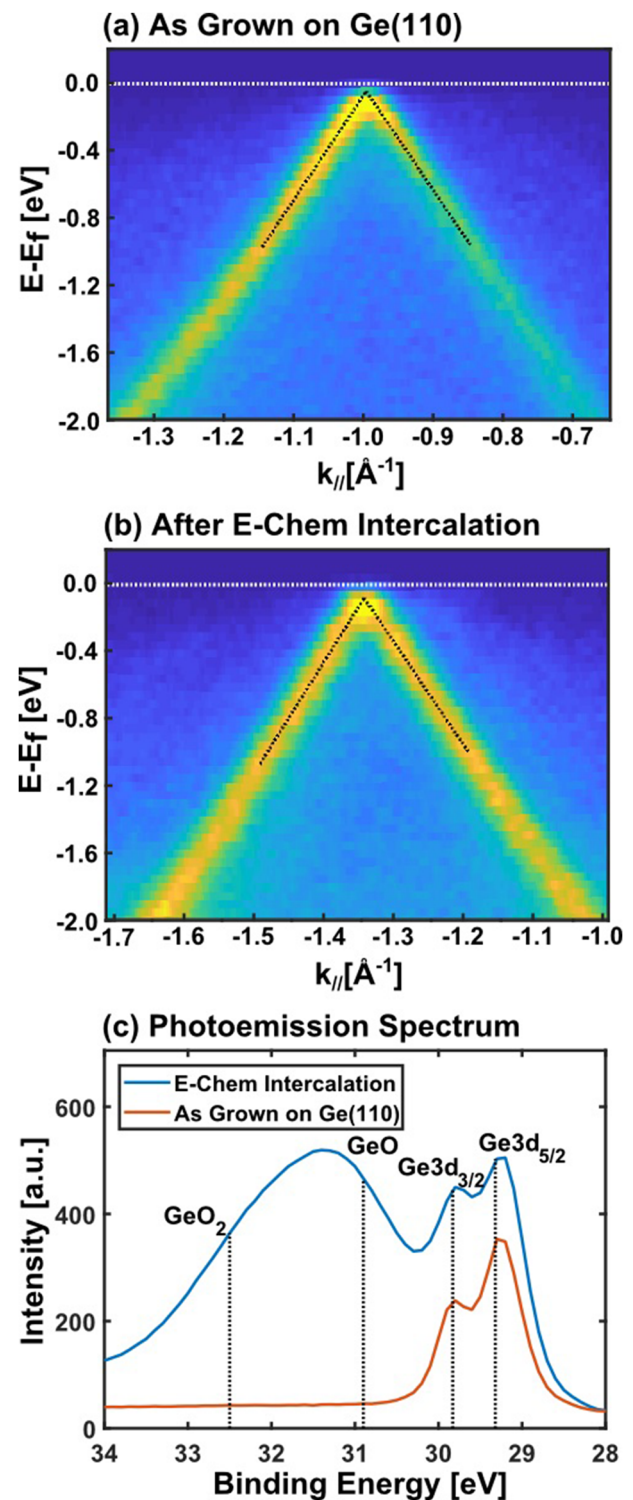

FIG. 2. NanoARPES analysis of (a) graphene as-grown on Ge(110) and (b) after electrochemical intercalation for 6 h at 1 V. (c) Photoemission spectra corresponding to (a) and (b).
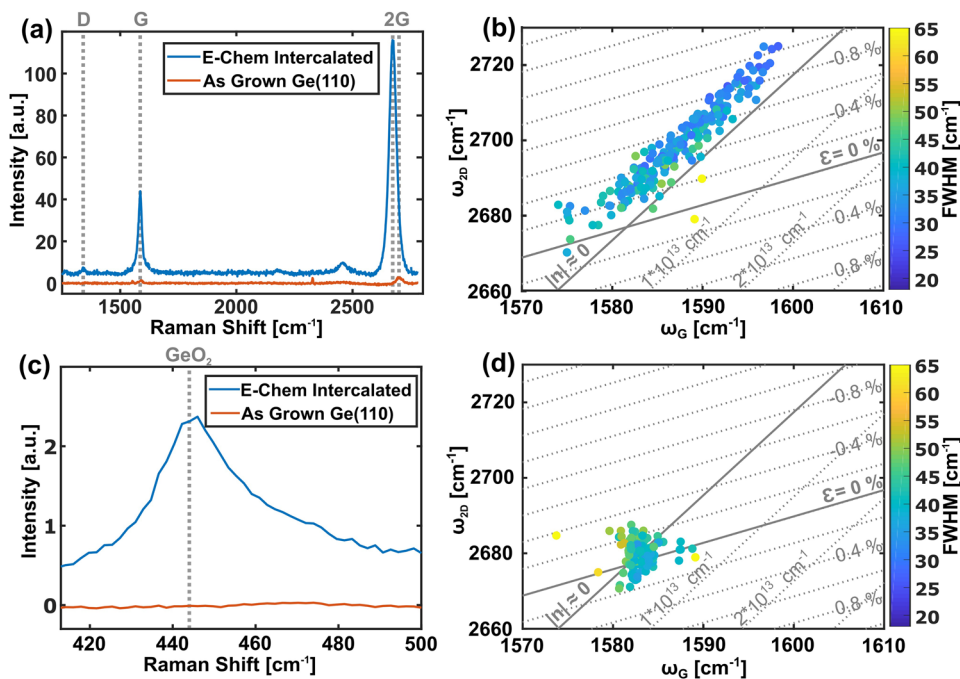
FIG. 3. Raman analysis of graphene on Ge(110) before and after electrochemical intercalation. (a) Graphene Raman peaks and (c) Ge oxide Raman signature. (b) and (d) scatter plots of the graphene Raman G peak position (ω_G) and 2D peak position (ω_{2D}) and full width half maximum (FWHM) of the 2D peak, where (b) was acquired on as-grown graphene on Ge(110) and (d) after electrochemical intercalation for 24 h.

Figures 3(b) and 3(d) show the Raman G-peak position (ω_G) vs 2D-peak position (ω_{2D}) for multiple locations across the sample to highlight the strain (ϵ) and charge transfer doping[17,77–79] ($|n|$) before and after electrochemical intercalation (see also the supplementary material, Figs. S8 and S9). Raman mapping on as-grown graphene on Ge(110) shows that graphene is under compressive strain with a large strain variation throughout the sample as highlighted by an average ω_{2D} = 2697 ± 12 cm^{-1} and ω_G = 1587 ± 5 cm^{-1}, in line with the previous literature.[32] This compressive strain is relaxed after intercalation, indicated by a shift of ω_{2D} by approximately 20 cm^{-1} to ω_{2D} = 2680 ± 3 cm^{-1}. Furthermore, Fig. 3(b) shows that as-grown graphene on Ge(110) is practically undoped, whereas for electrochemical intercalation approaches, the Raman signal indicates very low doping concentrations (ω_G = 1583 ± 1.6 cm^{-1}). This is consistent with the ARPES measurements above that indicated slightly increased p-type doping.

To understand the origin of this very low substrate induced doping and residual strain, we probe the structural interface between graphene and Ge oxide with helium ion microscopy (HIM) and atomic force microscopy (AFM). In comparison with scanning electron microscopy (SEM), HIM offers higher surface sensitivity combined with higher material contrast and resolution, as well as reduced imaging artifacts due to charging. Figure 4(a) shows HIM analysis of a sample area only partly covered by graphene so that the graphene/Ge oxide interface is revealed (highlighted by white arrows). The Ge oxide exhibits a regular pattern of nanoscale roughness. The graphene layer on top does not fully conform to this pattern and hence is partially free-standing. AFM allows us to resolve this surface topography more quantitatively. We find a Ge oxide surface roughness with graphene of approximately R_{RMS} = 6 nm (measured by AFM over an area of 1.5 × 1.5 μm^2). Such

surface roughening has been previously reported and arises due to the crystal structure of GeO$_2$ and oxide growth from nucleation sites with random orientation.[42,47] Oxide nucleation and growth can be observed *in situ*, as shown in Fig. S10. The onset of oxide growth is delayed [Figs. S10(a) and S10(b)] when comparing graphene covered to graphene uncovered regions due to the time required for the reactive species to intercalate. After intercalation, graphene covered regions oxidize more uniformly, highlighted by a more homogeneous color contrast [Figs. S10(c) and S10(f)] compared to uncovered regions where the oxide thickness varies throughout the sample.

ToF-SIMS was performed on the graphene grown on Ge(110) after electrochemical intercalation for 24 h to grow a thick Ge oxide layer (Fig. 5). 10 keV Cs$^+$ ion sputtering was used for depth profiling, over an extended period of time (10 000 s). The SIMS data show that there is an approximately 350 nm thick Ge oxide layer at the graphene-Ge interface for the given conditions (see Sec. IV in the supplementary material). The depth profile (supplementary material, Fig. S16) was averaged over an area of 150 × 150 μm^2. We do not observe a sharp interface between the Ge oxide and Ge in the depth profile. This can be explained by the microcrystalline structure of the Ge oxide, causing differences in oxide thicknesses across the sample as observed in the 3D depth profile image in Fig. 5(c) for the CsGeO$^+$ signal, as well as different crystal orientations that will have different sputter rates. The presence of graphene on the thick Ge oxide layer is confirmed by the C$_2^-$ ion image during more surface sensitive Ar cluster depth profiling from this sample, shown in Fig. S17.

Our results of electrochemical intercalation of graphene on Ge can be understood in the context of the electrochemical intercalation of graphite, where in contrast to other intercalation approaches,
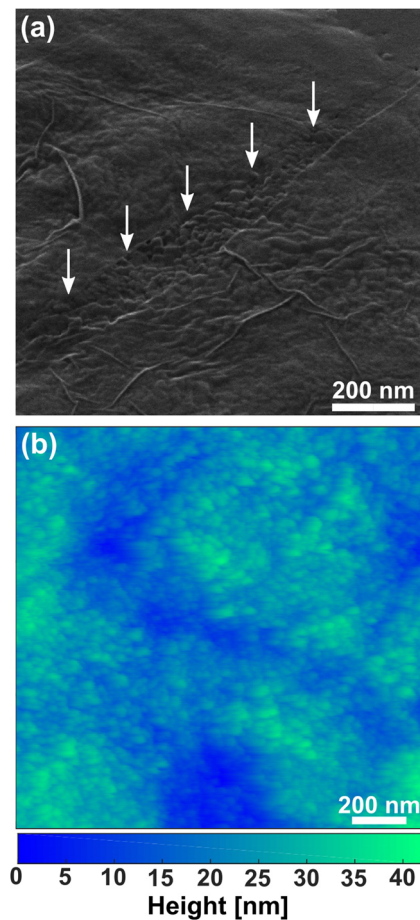
FIG. 4. (a) Helium ion microscope (HIM) image of a graphene layer on Ge oxide. White arrows indicate the edge of a tear in the graphene layer that leaves an uncovered Ge oxide area. (b) Atomic force microscope (AFM) image of graphene on Ge oxide [different region to (a)].
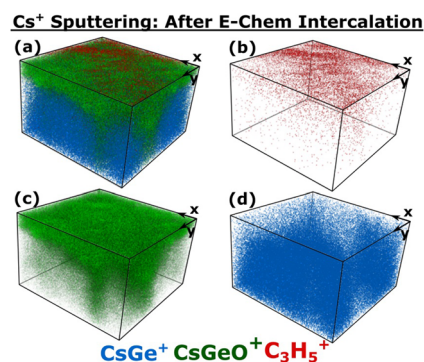

FIG. 5. 3D ToF-SIMS images of graphene on Ge (110) after electrochemical intercalation for 24 h using 10 keV Cs^+ ion depth profiling. The x and y dimensions of the 3D plot are $150 \times 150 \ \mu m^2$, and the z dimension is 3000 nm. Plot (a) shows the combined signal, whereas (b) shows $C_3H_5^+$ signal, (c) the $CsGeO^+$ signal, and (d) the $CsGe^+$ signal, representative of graphene, Ge oxide, and Ge substrate, respectively.

the electrochemical methodology can be performed at milder conditions. Furthermore, the electric field provides an additional driving force for molecules to intercalate, thereby significantly accelerating the process.[80,81] For graphene on Cu, mechanical decoupling of graphene from the catalyst substrate by oxidation has been shown to be a vital step for high quality, large area transfer from graphene on Cu.[10,12,82] As in the case of other graphene/metal interfaces, the graphene uncovered sample edge as well as defects in the graphene film can act as pathways for intercalants to diffuse into the graphene/Ge interface. Our oxidation approach would allow the translation of such transfer approaches to a Ge platform with the added advantage of being Cu free, which is crucial for CMOS integration.[83] Since epitaxial Ge films on Si wafers can be used, this is scalable to current Si wafer sizes.[28] Importantly, creation of a dielectric at the interface between Ge and graphene, as we have shown here, may also open the possibility for a transfer free graphene integration on a Si platform, where the intercalated dielectric is used as a gate dielectric. Furthermore, recent attempts to find a suitable dielectric layer for Ge based CMOS have investigated GeO_2 with a dielectric capping layer as protection.[54–56] Thus, the graphene layer on interface oxidized Ge could act as an atomically thin capping layer stabilizing the Ge oxide.

CONCLUSION

We have shown that by an electrochemical approach, graphene directly grown on Ge can be intercalated in a 0.25 N solution of anhydrous sodium acetate in glacial acetic acid at 1 V for 24 h and a 350 nm thick Ge oxide can be formed at the interface without damage to the graphene. This is despite the passivating nature of graphene on Ge in ambient conditions. The graphene defect density does not increase during electrochemical intercalation, and our ARPES and Raman measurements in fact show that the CVD induced strain in the graphene layer can be released as graphene is decoupled from the Ge substrate.

METHODS

If not otherwise stated, graphene was synthesized on undoped (>50 Ω cm) single crystal Ge(110) substrates (0.5 mm thickness, Pi Kem Ltd.) in a commercial Aixtron Black Magic Pro Reactor (base pressure 5×10^{-2} mbar). The as-received Ge substrates were loaded into the CVD reactor without further treatment. The temperature was ramped to approximately 900 °C (as measured by using a pyrometer against a graphite plate) at a rate of 100 °C/min in a H_2 atmosphere. The substrates were annealed for 90 min at 900 °C, followed by CH_4 injection (H_2:CH_4 flow rate ratio was 26:1 SCCM) for a time period (t_g) of 120 min. After the growth, the chamber was cooled in a H_2 atmosphere. The chamber pressure during all stages was 50 mbar.

Electrochemical graphene intercalation was performed in a 0.25 N solution of anhydrous sodium acetate in glacial acetic acid[53] using a Pt wire as cathode and the Ge/graphene substrate as anode with 1 V potential difference for a time of 6–24 h and subsequent rinsing in glacial acetic acid, blow drying with N_2, and heating at 150 °C on a hotplate for 1 h.

Nanoresolution angle-resolved photoelectron spectroscopy (nanoARPES) was carried out at the I05-ARPES beamline of

Diamond Light Source (Didcot, UK). Spatial resolution is achieved by focusing the photon beam into a spot with a diameter of 600 nm. The Fermi level reference was measured on a film of polycrystalline gold. Before ARPES, all samples were annealed in ultrahigh vacuum (below 1×10^{-9} mbar) for 2 h at 150 °C and ARPES measurements were performed at a temperature of 30 K (−243 °C). Helium Ion Microscopy (HIM) was performed using a Zeiss Orion NanoFab. Secondary electron images were collected using a scanning focused beam of 25 keV He$^+$ ions with the sample tilted at 45°. Scanning electron microscopy (SEM) pictures were taken with a Carl Zeiss SIGMA VP at an acceleration voltage of 2 kV.

SUPPLEMENTARY MATERIAL

See supplementary material for further information on CVD growth details; SEM and TEM characterization; additional Raman and SIMS data; and details on wet and gas phase intercalation.

REFERENCES

[1] K. S. Novoselov, A. Mishchenko, A. Carvalho, and A. H. C. Neto, "2D materials and van der Waals heterostructures," Science **353**, aac9439 (2016).

[2] A. K. Geim and I. V. Grigorieva, "Van der Waals heterostructures," Nature **499**, 419–425 (2013).

[3] P. Ajayan, P. Kim, and K. Banerjee, "Two-dimensional van der Waals materials," Phys. Today **69**(9), 38–44 (2016).

[4] X. Xu, Z. Zhang, J. Dong, D. Yi, J. Niu, M. Wu, L. Lin, R. Yin, M. Li, J. Zhou, S. Wang, J. Sun, X. Duan, P. Gao, Y. Jiang, X. Wu, H. Peng, R. S. Ruoff, Z. Liu, D. Yu, E. Wang, F. Ding, and K. Liu, "Ultrafast epitaxial growth of metre-sized single-crystal graphene on industrial Cu foil," Sci. Bull. **62**, 1074–1080 (2017).

[5] R. S. Weatherup, C. Baehtz, B. Dlubak, B. C. Bayer, P. R. Kidambi, R. Blume, R. Schloegl, and S. Hofmann, "Introducing carbon diffusion barriers for uniform, high-quality graphene growth from solid sources," Nano Lett. **13**, 4624–4631 (2013).

[6] A. Cabrero-Vilatela, R. S. Weatherup, P. Braeuninger-Weimer, S. Caneva, and S. Hofmann, "Towards a general growth model for graphene CVD on transition metal catalysts," Nanoscale **8**, 2149–2158 (2016).

[7] S. Caneva, R. S. Weatherup, B. C. Bayer, R. Blume, A. Cabrero-Vilatela, P. Braeuninger-Weimer, M.-B. Martin, R. Wang, C. Baehtz, R. Schlögl, J. C. Meyer, and S. Hofmann, "Controlling catalyst bulk reservoir effects for monolayer hexagonal boron nitride CVD," Nano Lett. **16**, 1250–1261 (2016).

[8] P. Braeuninger-Weimer, B. Brennan, A. J. Pollard, and S. Hofmann, "Understanding and controlling Cu catalyzed graphene nucleation: The role of impurities, roughness and oxygen scavenging," Chem. Mater. **28**, 8905–8915 (2016).

[9] Y. Wang, Y. Zheng, X. Xu, E. Dubuisson, Q. Bao, J. Lu, and K. P. Loh, "Electrochemical delamination of CVD-grown graphene film: Toward the recyclable use of copper catalyst," ACS Nano **5**, 9927–9933 (2011).

[10] R. Wang, P. R. Whelan, P. Braeuninger-Weimer, S. Tappertzhofen, J. A. Alexander-webber, Z. A. Van-veldhoven, P. R. Kidambi, B. S. Jessen, T. J. Booth, P. Boggild, and S. Hofmann, "Catalyst interface engineering for improved 2D film lift-off and transfer," ACS Appl. Mater. Interfaces **8**, 33072–33082 (2016).

[11] R. Wang, D. G. Purdie, Y. Fan, F. C. Massabuau, P. Braeuninger-Weimer, O. J. Burton, R. Blume, R. Schloegl, A. Lombardo, R. S. Weatherup, and S. Hofmann, "A peeling approach for integrated manufacturing of large monolayer h-BN crystals," ACS Nano **13**, 2114 (2019).

[12] L. Banszerus, M. Schmitz, S. Engels, J. Dauber, M. Oellers, F. Haupt, K. Watanabe, T. Taniguchi, B. Beschoten, and C. Stampfer, "Ultrahigh-mobility graphene devices from chemical vapor deposition on reusable copper," Sci. Adv. **1**, e1500222 (2015).

[13] G. Giovannetti, P. A. Khomyakov, G. Brocks, V. M. Karpan, J. V. D. Brink, and P. J. Kelly, "Doping graphene with metal contacts," Phys. Rev. Lett. **101**, 026803 (2008).

[14] M. B. Martin, B. Dlubak, R. S. Weatherup, M. Piquemal-Banci, H. Yang, R. Blume, R. Schloegl, S. Collin, F. Petroff, S. Hofmann, J. Robertson, A. Anane, A. Fert, and P. Seneor, "Protecting nickel with graphene spin-filtering membranes: A single layer is enough," Appl. Phys. Lett. **107**, 012408 (2015).

[15] J. A. Alexander-Webber, A. A. Sagade, A. I. Aria, Z. A. Van-Veldhoven, A. Cabrero-Vilatela, P. Braeuninger-Weimer, R. Wang, J. Sui, M. R. Connolly, M.-B. Martin, and S. Hofmann, "Hysteresis-free encapsulated CVD graphene transistors via interface engineering of atomic layer deposited oxide," 2D Mater. **4**, 011008 (2016).

[16] B. Dlubak, M.-B. Martin, R. S. Weatherup, H. Yang, C. Deranlot, R. Blume, R. Schloegl, A. Fert, A. Anane, S. Hofmann, P. Seneor, and J. Robertson, "Graphene-passivated nickel as an oxidation-resistant spin polarized electrode," ACS Nano **6**, 10930–10934 (2012).

[17] L. Banszerus, H. Janssen, M. Otto, A. Epping, T. Taniguchi, K. Watanabe, B. Beschoten, D. Neumaier, and C. Stampfer, "Identifying suitable substrates for high-quality graphene-based heterostructures," 2D Mater. **4**, 025030 (2016).

[18] R. Raj, S. C. Maroo, and E. N. Wang, "Wettability of graphene," Nano Lett. **13**, 1509 (2013).

[19] A. I. Aria, P. R. Kidambi, R. S. Weatherup, L. Xiao, J. A. Williams, and S. Hofmann, "Time evolution of the wettability of supported graphene under ambient air exposure," J. Phys. Chem. C **120**, 2215 (2016).

[20] J. Rafiee, X. Mi, H. Gullapalli, A. V. Thomas, F. Yavari, Y. Shi, P. M. Ajayan, and N. A. Koratkar, "Wetting transparency of graphene," Nat. Mater. **11**, 217–222 (2012).

[21] Y. Kim, S. S. Cruz, K. Lee, B. O. Alawode, C. Choi, Y. Song, J. M. Johnson, C. Heidelberger, W. Kong, S. Choi, K. Qiao, I. Almansouri, E. A. Fitzgerald, J. Kong, A. M. Kolpak, J. Hwang, and J. Kim, "Remote epitaxy through graphene enables two-dimensional material-based layer transfer," Nature **544**, 340–343 (2017).

[22] R. S. Weatherup, L. D'Arsié, A. Cabrero-Vilatela, S. Caneva, R. Blume, J. Robertson, R. Schloegl, and S. Hofmann, "Long-term passivation of strongly interacting metals with single-layer graphene," J. Am. Chem. Soc. **137**, 14358–14366 (2015).

[23] S. Böhm, "Graphene against corrosion," Nat. Nanotechnol. **9**, 741–742 (2014).

[24] D. Luo, X. You, B.-W. Li, X. Chen, H. J. Park, M. Jung, T. Y. Ko, K. Wong, M. Yousaf, X. Chen, M. Huang, S. H. Lee, Z. Lee, H.-J. Shin, S. Ryu, S. K. Kwak, N. Park, R. R. Bacsa, W. Bacsa, and R. S. Ruoff, "Role of graphene in water-assisted oxidation of copper in relation to dry transfer of graphene," Chem. Mater. **29**, 4546–4556 (2017).

[25] P. R. Whelan, B. S. Jessen, R. Wang, B. Luo, A. C. Stoot, D. M. A. Mackenzie, P. Braeuninger-Weimer, A. Jouvray, L. Prager, L. Camilli, S. Hofmann, P. Bøggild, and T. J. Booth, "Raman spectral indicators of catalyst decoupling for transfer of CVD grown 2D materials," Carbon **117**, 75–81 (2017).

[26] A.-Y. Lu, S.-Y. Wei, C.-Y. Wu, Y. Hernandez, T.-Y. Chen, T.-H. Liu, C.-W. Pao, F.-R. Chen, L.-J. Li, and Z.-Y. Juang, "Decoupling of CVD graphene by controlled oxidation of recrystallized Cu," RSC Adv. **2**, 3008 (2012).

[27] J.-H. Lee, E. K. Lee, W.-J. Joo, Y. Jang, B.-S. Kim, J. Y. Lim, S.-H. Choi, S. J. Ahn, J. R. Ahn, M.-H. Park, C.-W. Yang, B. L. Choi, S.-W. Hwang, and D. Whang, "Wafer-scale growth of single-crystal monolayer graphene on reusable hydrogen-terminated germanium," Science **344**, 286–289 (2014).

[28] M. Lukosius, J. Dabrowski, J. Kitzmann, O. Fursenko, M. Lisker, F. Akhtar, S. Schulze, G. Lippert, Y. Yamamoto, M. A. Schubert, H.-M. Krause, A. Wolff, A. Mai, T. Schroeder, and G. Lupina, "Metal-free CVD graphene synthesis on 200 Mm Ge/Si (100) substrates," ACS Appl. Mater. Interfaces **8**, 33786–33793 (2016).

[29] G. Wang, M. Zhang, Y. Zhu, G. Ding, D. Jiang, Q. Guo, S. Liu, X. Xie, P. K. Chu, Z. Di, and X. Wang, "Direct growth of graphene film on germanium substrate," Sci. Rep. **3**, 2465 (2013).

[30] M. Lukosius, G. Lippert, J. Dabrowski, J. Kitzmann, M. Lisker, P. Kulse, A. Krüger, O. Fursenko, I. Costina, A. Trusch, Y. Yamamoto, A. Wolff, A. Mai, T. Schroeder, and G. Lupina, "Graphene synthesis and processing on Ge substrates," ECS Trans. **75**, 533–540 (2016).

[31] J. Dai, D. Wang, M. Zhang, T. Niu, A. Li, M. Ye, S. Qiao, G. Ding, X. Xie, Y. Wang, P. K. Chu, Q. Yuan, Z. Di, X. Wang, F. Ding, and B. I. Yakobson, "How graphene islands are unidirectionally aligned on Ge(110) surface," Nano Lett. **16**, 3160–3165 (2016).

[32] B. Kiraly, R. M. Jacobberger, A. J. Mannix, G. P. Campbell, M. J. Bedzyk, M. S. Arnold, M. C. Hersam, and N. P. Guisinger, "Electronic and mechanical properties of graphene–germanium interfaces grown by chemical vapor deposition," Nano Lett. **15**, 7414–7420 (2015).

[33] K. V. Emtsev, A. Bostwick, K. Horn, J. Jobst, G. L. Kellogg, L. Ley, J. L. McChesney, T. Ohta, S. A. Reshanov, J. Röhrl, E. Rotenberg, A. K. Schmid, D. Waldmann, H. B. Weber, and T. Seyller, "Towards wafer-size graphene layers by atmospheric pressure graphitization of silicon carbide," Nat. Mater. **8**, 203–207 (2009).

[34] W. A. de Heer, C. Berger, M. Ruan, M. Sprinkle, X. Li, Y. Hu, B. Zhang, J. Hankinson, and E. Conrad, "Large area and structured epitaxial graphene produced by confinement controlled sublimation of silicon carbide," Proc. Natl. Acad. Sci. U. S. A. **108**, 16900–16905 (2011).

[35] S. Oida, F. R. McFeely, J. B. Hannon, R. M. Tromp, M. Copel, Z. Chen, Y. Sun, D. B. Farmer, and J. Yurkas, "Decoupling graphene from SiC(0001) via oxidation," Phys. Rev. B **82**, 041411 (2010).

[36] C. Riedl, C. Coletti, T. Iwasaki, A. A. Zakharov, and U. Starke, "Quasi-free-standing epitaxial graphene on SiC obtained by hydrogen intercalation," Phys. Rev. Lett. **103**, 246804 (2009).

[37] W. Strupinski, K. Grodecki, A. Wysmolek, R. Stepniewski, T. Szkopek, P. E. Gaskell, and A. Gr, "Graphene epitaxy by chemical vapor deposition on SiC," Nano Lett. **11**, 1786–1791 (2011).

[38] R. R. Delgado, R. M. Jacobberger, S. S. Roy, S. Mangu, M. S. Arnold, F. Cavallo, and M. G. Lagally, "Passivation of germanium by graphene passivation of germanium by graphene," ACS Appl. Mater. Interfaces **9**, 17629–17636 (2017).

[39] G. P. Campbell, B. Kiraly, R. M. Jacobberger, A. J. Mannix, M. S. Arnold, M. C. Hersam, N. P. Guisinger, and M. J. Bedzyk, "Epitaxial graphene-encapsulated surface reconstruction of Ge(110)," Phys. Rev. Mater. **2**, 044004 (2018).

[40] A. W. Laubengayer and D. S. Morton, "The polymorphism of germanium dioxide," J. Am. Chem. Soc. **54**, 2303 (1932).

[41] M. Pourbaix, *Atlas of Electrochemical Equilibria in Aqueous Solutions* (Pergamon Press, 1966).

[42] F. L. Edelman, L. N. Alexandrov, L. I. Fedina, and V. S. Latuta, "The structure of GeO$_2$ films grown on Ge," Thin Solid Films **34**, 107–110 (1976).

[43] Q. Xie, S. Deng, M. Schaekers, D. Lin, M. Caymax, A. Delabie, X.-P. Qu, Y.-L. Jiang, D. Deduytsche, and C. Detavernier, "Germanium surface passivation and atomic layer deposition of high-k dielectrics—A tutorial review on Ge-based MOS capacitors," Semicond. Sci. Technol. **27**, 074012 (2012).

[44] J. Grzonka, I. Pasternak, P. P. Michałowski, V. Kolkovsky, and W. Strupinski, "Influence of hydrogen intercalation on graphene/Ge(0 0 1)/Si(0 0 1) interface," Appl. Surf. Sci. **447**, 582–586 (2018).

[45] D. Zhou, Z. Niu, and T. Niu, "Surface reconstruction of germanium: Hydrogen intercalation and graphene protection," J. Phys. Chem. C **122**, 21874 (2018).

[46] P. Dabrowski, M. Rogala, I. Pasternak, J. Baranowski, W. Strupinski, M. Kopciuszynski, R. Zdyb, M. Jalochowski, I. Lutsyk, and Z. Klusek, "The study of the interactions between graphene and Ge(001)/Si(001)," Nano Res. **10**, 3648 (2017).

[47] E. Valyocsik, "Germanium oxidation in nitric acid," J. Electrochem. Soc. **114**, 176 (1967).

[48] S. Kalem, Ö. Arthursson, and I. Romandic, "Transformation of germanium to fluogermanates," Appl. Phys. A **98**, 423–428 (2010).

[49] L. M. Dennis, K. M. Tressler, and F. E. Hance, "Germanium. VI. Metallic germanium. Reduction of germanium dioxide. Preparation of fused germanium. Physical and chemical properties," J. Am. Chem. Soc. **45**, 2033–2047 (1923).

[50] M. C. Cretella and H. C. Gatos, "The reaction of germanium with aqueous solutions," J. Electrochem. Soc. **105**, 654 (1958).

[51] O. J. Gregory, L. A. Pruitt, E. E. Crisman, C. Roberts, and P. J. Stiles, "Native oxides formed on single-crystal germanium by wet chemical reactions," J. Electrochem. Soc. **135**, 923–929 (1988).

[52] B. Onsia, M. Caymax, T. Conard, S. De Gendt, F. De Smedt, A. Delabie, C. Gottschalk, M. M. Heyns, M. Green, S. Lin, P. W. Mertens, W. Tsai, and C. Vinckier, "On the application of a thin ozone based wet chemical oxide as an interface for ALD high-k deposition," Solid State Phenom. **103-104**, 19–22 (2005).

[53] S. Zwerdling and S. Sheff, "The growth of anodic oxide films on germanium," J. Electrochem. Soc. **107**, 338–342 (1960).

[54] M. Kobayashi, G. Thareja, M. Ishibashi, Y. Sun, P. Griffin, J. McVittie, P. Pianetta, K. Saraswat, and Y. Nishi, "Radical oxidation of germanium for interface gate dielectric GeO$_2$ formation in metal-insulator-semiconductor gate stack," J. Appl. Phys. **106**, 104117 (2009).

[55] K. Kita, S. Suzuki, H. Nomura, T. Takahashi, T. Nishimura, and A. Toriumi, "Direct evidence of GeO volatilization from GeO$_2$/Ge and impact of its suppression on GeO$_2$/Ge metal-insulator-semiconductor characteristics," Jpn. J. Appl. Phys., Part 1 **47**, 2349–2353 (2008).

[56] Y. Fukuda, T. Ueno, S. Hirono, and S. Hashimoto, "Electrical characterization of germanium oxide/germanium interface prepared by electron-cyclotron-resonance plasma irradiation," Jpn. J. Appl. Phys., Part 1 **44**, 6981–6984 (2005).

[57] P. C. Rogge, M. E. Foster, J. M. Wofford, K. F. McCarty, N. C. Bartelt, and O. D. Dubon, "On the rotational alignment of graphene domains on Ge(110) and Ge(111)," MRS Commun. **5**, 539 (2015); e-print arXiv:1507.00083.

[58] J. Dabrowski, G. Lippert, J. Avila, J. Baringhaus, I. Colambo, Y. S. Dedkov, F. Herziger, G. Lupina, J. Maultzsch, T. Schaffus, T. Schroeder, M. Kot, C. Tegenkamp, D. Vignaud, and M. C. Asensio, "Understanding the growth mechanism of graphene on Ge/Si(001) surfaces," Sci. Rep. **6**, 31639 (2016).

[59] T. Sasada, Y. Nakakita, M. Takenaka, and S. Takagi, "Surface orientation dependence of interface properties of GeO$_2$/Ge metal-oxide-semiconductor structures fabricated by thermal oxidation," J. Appl. Phys. **106**, 073716 (2009).

[60] J. T. Law and P. S. Meigs, "Rates of oxidation of germanium," J. Electrochem. Soc. **104**, 154 (1957).

[61] A. Varykhalov, J. Sánchez-Barriga, A. M. Shikin, C. Biswas, E. Vescovo, A. Rybkin, D. Marchenko, and O. Rader, "Electronic and magnetic properties of quasifreestanding graphene on Ni," Phys. Rev. Lett. **101**, 157601 (2008).

[62] P. Sutter, J. T. Sadowski, and E. A. Sutter, "Chemistry under cover: Tuning metal-graphene interaction by reactive intercalation," J. Am. Chem. Soc. **132**, 8175–8179 (2010).

[63] R. Blume, P. R. Kidambi, B. C. Bayer, R. S. Weatherup, Z.-J. Wang, G. Weinberg, M.-G. Willinger, M. Greiner, S. Hofmann, A. Knop-Gericke, and R. Schlögl, "The influence of intercalated oxygen on the properties of graphene on polycrystalline Cu under various environmental conditions," Phys. Chem. Chem. Phys. **16**, 25989–26003 (2014).

[64] P. R. Kidambi, B. C. Bayer, R. Blume, Z.-J. Wang, C. Baehtz, R. S. Weatherup, M.-G. Willinger, R. Schloegl, and S. Hofmann, "Observing graphene grow: Catalyst-graphene interactions during scalable graphene growth on polycrystalline copper," Nano Lett. **13**, 4769–4778 (2013).

[65] R. Larciprete, S. Ulstrup, P. Lacovig, M. Dalmiglio, M. Bianchi, F. Mazzola, L. Hornekær, F. Orlando, A. Baraldi, P. Hofmann, and S. Lizzit, "Oxygen switching of the epitaxial graphene-metal interaction," ACS Nano **6**, 9551–9558 (2012).

[66] J. Moulder, W. Stickle, P. E. Sobol, and D. K. Bomben, *Handbook of X-Ray Photoelectron Spectroscopy* (Physical Electronics Division, Perkin-Elmer Corporation, 1992).

[67] M. Micoulaut, L. Cormier, and G. S. Henderson, "The structure of amorphous, crystalline and liquid GeO_2," J. Phys.: Condens. Matter **18**, R753–R784 (2006).

[68] R. Zhou, S. Yasuda, H. Minamimoto, and K. Murakoshi, "Sensitive Raman probe of electronic interactions between monolayer graphene and substrate under electrochemical potential control," ACS Omega **3**, 2322 (2018).

[69] I. Palacio, G. Otero-Irurueta, C. Alonso, J. I. Martínez, E. López-Elvira, I. Muñoz-Ochando, H. J. Salavagione, M. F. López, M. García-Hernández, J. Méndez, G. J. Ellis, and J. A. Martín-Gago, "Chemistry below graphene: Decoupling epitaxial graphene from metals by potential-controlled electrochemical oxidation," Carbon **129**, 837–846 (2018).

[70] P. W. Sutter, J.-I. Flege, and E. A. Sutter, "Epitaxial graphene on ruthenium," Nat. Mater. **7**, 406–411 (2008).

[71] D. Y. Usachov, V. Y. Davydov, V. S. Levitskii, V. O. Shevelev, D. Marchenko, B. V. Senkovskiy, O. Y. Vilkov, A. G. Rybkin, L. V. Yashina, E. V. Chulkov, I. Y. Sklyadneva, R. Heid, K.-P. Bohnen, C. Laubschat, and D. V. Vyalikh, "Raman spectroscopy of lattice-matched graphene on strongly interacting metal surfaces," ACS Nano **11**, 6336–6345 (2017).

[72] A. Allard and L. Wirtz, "Graphene on metallic substrates: Suppression of the Kohn anomalies in the phonon dispersion," Nano Lett. **10**, 4335–4340 (2010).

[73] P. Blake, E. W. Hill, A. H. Castro Neto, K. S. Novoselov, D. Jiang, R. Yang, T. J. Booth, and A. K. Geim, "Making graphene visible," Appl. Phys. Lett. **91**, 063124 (2007).

[74] C. Liu, Y. Ma, W. Li, L. Dai, C. Liu, Y. Ma, W. Li, and L. Dai, "The evolution of Raman spectrum of graphene with the thickness of SiO_2 capping layer on Si substrate," Appl. Phys. Lett. **103**, 213103 (2013).

[75] Y. Y. Wang, Z. H. Ni, Z. X. Shen, H. M. Wang, and Y. H. Wu, "Interference enhancement of Raman signal of graphene," Appl. Phys. Lett. **92**, 043121 (2008).

[76] R. Ramírez-Jíménez, L. Álvarez-Fraga, F. Jimenez-Villacorta, E. Climent-Pascual, C. Prieto, and A. De Andrés, "Interference enhanced Raman effect in graphene bubbles," Carbon **105**, 556–565 (2016).

[77] C. Neumann, S. Reichardt, P. Venezuela, M. Drögeler, L. Banszerus, M. Schmitz, K. Watanabe, T. Taniguchi, F. Mauri, B. Beschoten, S. V. Rotkin, C. Stampfer, C. Neumann, S. Reichardt, and M. Dro, "Raman spectroscopy as probe of nanometre-scale strain variations in graphene," Nat. Commun. **6**, 8429 (2015).

[78] J. E. Lee, G. Ahn, J. Shim, Y. S. Lee, and S. Ryu, "Optical separation of mechanical strain from charge doping in graphene," Nat. Commun. **3**, 1024 (2012).

[79] A. Das, S. Pisana, B. Chakraborty, S. Piscanec, S. K. Saha, U. V. Waghmare, K. S. Novoselov, H. R. Krishnamurthy, A. K. Geim, A. C. Ferrari, and A. K. Sood, "Monitoring dopants by Raman scattering in an electrochemically top-gated graphene transistor," Nat. Nanotechnol. **3**, 210–215 (2008).

[80] A. M. Abdelkader, A. J. Cooper, R. A. W. Dryfe, and I. A. Kinloch, "How to get between the sheets: A review of recent works on the electrochemical exfoliation of graphene materials from bulk graphite," Nanoscale **7**, 6944 (2015).

[81] A. Ambrosi and M. Pumera, "Exfoliation of layered materials using electrochemistry," Chem. Soc. Rev. **47**, 7213–7224 (2018).

[82] A. Shivayogimath, P. R. Whelan, D. M. A. Mackenzie, B. Luo, D. Huang, M. Wang, L. Gammelgaard, H. Shi, R. S. Ruoff, P. Bøggild, and T. J. Booth, "Do-it-yourself transfer of large-area graphene using an office laminator and water," Chem. Mater. **31**, 2328 (2019).

[83] G. Lupina, J. Kitzmann, I. Costina, M. Lukosius, C. Wenger, A. Wolff, S. Vaziri, M. Ostling, I. Pasternak, A. Krajewska, W. Strupinski, S. Kataria, A. Gahoi, M. C. Lemme, G. Ruhl, G. Zoth, O. Luxenhofer, and W. Mehr, "Residual metallic contamination of transferred chemical vapor deposited graphene," ACS Nano **9**, 4776–4785 (2015).